Supplementary Material

Late Holocene uplift of Rhodes, Greece: evidence for a large tsunamigenic earthquake and the implications for the tectonics of the eastern Hellenic Trench System

Andy Howell, James Jackson, Philip England, Thomas Higham and Costas Synolakis

This supplementary section contains details of the fit of various models to the observed uplift. It should be noted that these plots show examples of trade-offs rather than an exhaustive documentation of our search of parameter space. For example, a trade-off between distance from the coast and maximum depth of rupture is illustrated here with dip fixed, because this makes it easier to see the pattern. We have checked that the pattern applies when the dip is fixed at other values too, but do not publish all the relevant plots here for the sake of brevity.

S1 Choice of unacceptable misfit

In Section 4.2 of the main text, we set 40 cm as an upper limit for an acceptable RMS misfit of a fault model to the data. This may appear slightly counter-intuitive, since we also draw error bars of $\pm$60 cm on the plots at the base of Figure 6, suggesting that we are not certain of the elevation of any of the palæoshorelines relative to sea level at the time of uplift more accurately than this (which is true).

There are multiple sources of uncertainty in the estimates of palæoshoreline uplift, dominated by uncertainty in late Holocene eustatic sea-level history, a $\sim$20 cm uncertainty associated with modern tidal variations, and some possible small measurement errors. Nevertheless, we are confident that the estimates used are correct to within 1 m, especially where uplift is higher at the northern end of Rhodes.

Figure S1 shows the variation in misfit for individual points with dip and distance from the coast. Distance from the coast is allowed to vary from 0 to 30 km across strike (bearing 115°), and dip is allowed to vary from 20-60°. For simplicity, fault length is fixed at 60 km, strike is 205° and slip vector is 115°, although the same patterns of misfit still hold true if the parameters we have fixed are allowed to vary within the ranges specified in Table 2 in the main text. The fault ruptures from the surface to 40 km depth, and the SW end of the fault is constrained to lie on a bearing of 115° from Lindos (0 km along strike).

The presence of individual misfits of up to 0.7 m for corresponding overall RMS misfits of $<$0.25 m is our reason for choosing 0.4 m as an upper limit for acceptable RMS misfit. RMS misfit is dominated by the sites at the northern end of Rhodes, while sites at the southern end generally have a very low misfit to the models.

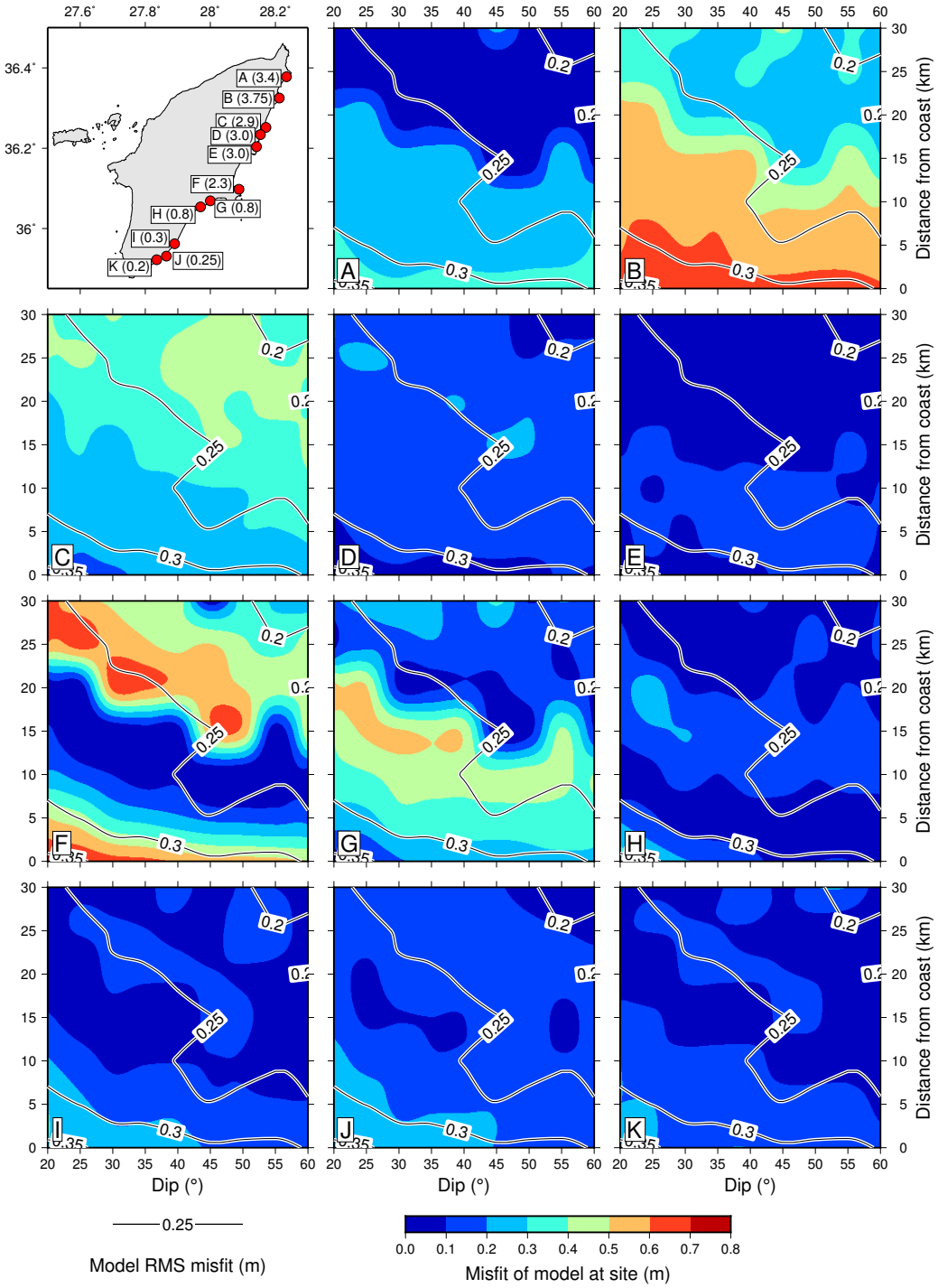

Figure S1: Variation of absolute misfits at individual sites (shown by the letters on the map) where uplift was observed with dip and distance from the coast. Black lines show contours of overall RMS misfit for the same models.
Fault length is fixed at 60 km, strike is 205° and slip vector is 115°. The fault ruptures from the surface to 40 km depth, and the SW end of the fault is constrained to lie on a bearing of 115° from Lindos (0 km along strike). Rake is fixed at 90°.

S2 Trade-offs between parameters

The points where palæoshoreline elevations were measured all fall close to a line along the SE coast of Rhodes (see Figure 3, main text; map in Figure S1). Several source parameters are poorly constrained because of this (the dip, for example), and this leads to the trade-offs between parameters listed below.

S2.1 Dip and magnitude of slip

Figure S2(a) shows the variation between dip and magnitude of best-fitting slip for varying distances from the coast. For faults above 20° dip, for a given distance from the coast, best-fitting slip increases with dip. Figure S2(b) shows how this slip compares with RMS misfit.

S2.2 Magnitude of slip and distance of the fault from the coast

Figure S2(a) also shows that for a given dip, slip increases with distance from the coast.

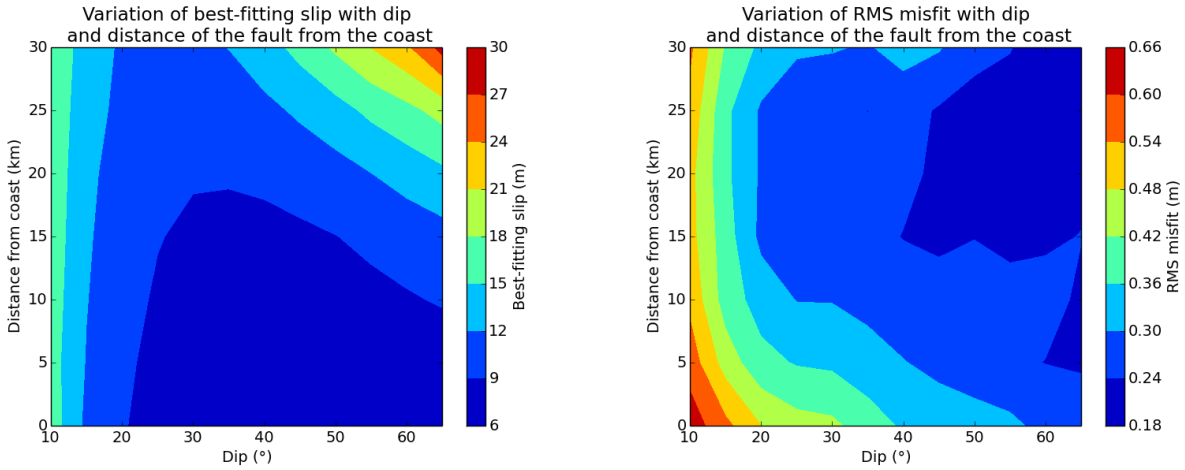

(a) (b)

Figure S2: Illustration of trade-offs between slip, dip and distance of the fault from the coast. (a) shows the variation in best-fitting slip, with all parameters apart from dip and distance from the coast fixed. The fault is constrained to strike at 205°; rupture is from the surface to 40 km depth; the length of the fault is 60 km and the SW end is constrained to lie on a bearing of 115° from Lindos (0 km along strike). Rake is fixed at 90°.

S2.3 Distance from the coast and depth of faulting

Figure S3 shows that for a fixed dip of 40° and a maximum depth of rupture of 20 km, the only models with an RMS misfit <0.5 m are 10 km from the coast. Fault models that rupture to a greater depth are able to fit the data satisfactorily with the fault further from the coast. This pattern also holds true for other dips.

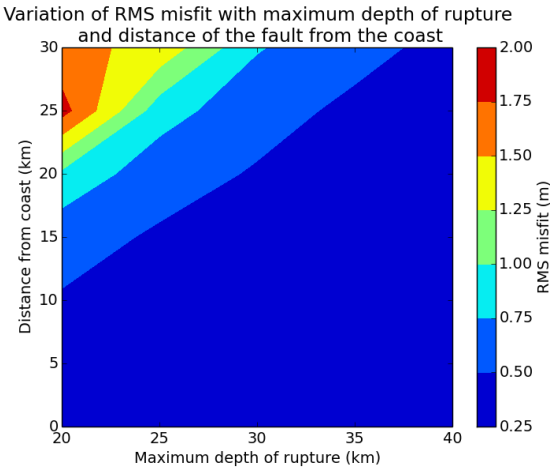

Figure S3: Illustration of trade-offs between RMS misfit, distance of the fault from the coast and maximum depth of rupture. The fault is constrained to strike at 205° and dip at 40°; rupture is from the surface to the depth specified; the length of the fault is 60 km and the SW end is constrained to lie on a bearing of 115° from Lindos (0 km along strike). Rake is fixed at 90°.

S2.4 Fault length and magnitude of slip

Figure S4(a) shows that the best-fitting slip changes dramatically with distance from the coast, but not significantly with length. Figure S4(b) shows variation of misfit with length and distance from the coast. This shows that faults over ∼50 km length are able to fit the data at most distances from the coast.

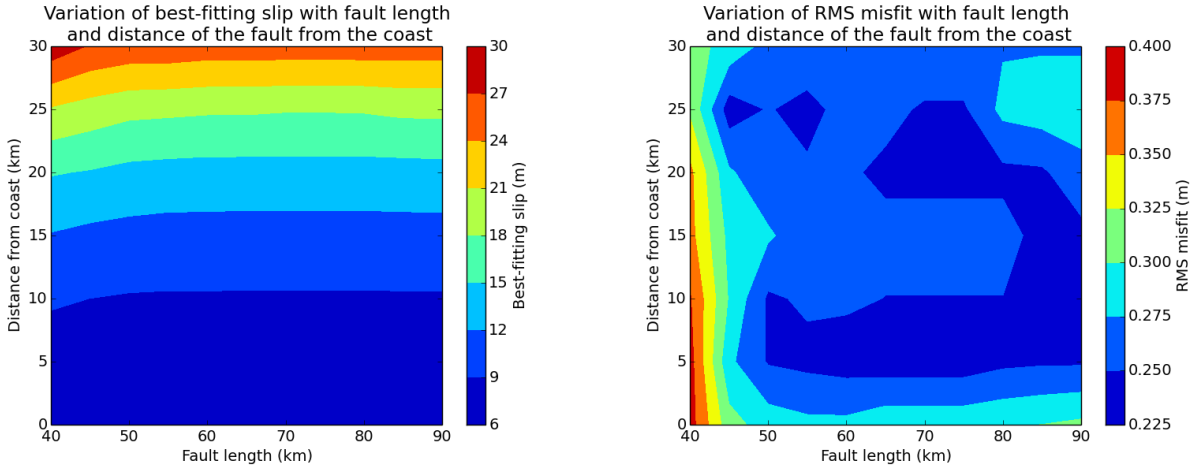

(a) (b)

Figure S4: Illustration of trade-offs between slip, dip and distance of the fault from the coast. (a) shows the variation in best-fitting slip, with all parameters apart from length and distance from the coast fixed. (b) shows variation in RMS misfit over the same region of parameter space. The fault is constrained to strike at 205° and dip at 60°; rupture is from the surface to 40 km and the SW end is constrained to lie on a bearing of 115° from Lindos (0 km along strike). Rake is fixed at 90°.

S3 Faults with a NE–SW slip vector

The fault models discussed in the supplementary material so far have their strike and slip vector fixed at 205° and 115° respectively; they are pure reverse faults with a strike that is parallel to the contours of bathymetry and an azimuth of slip vector perpendicular to this. If we assume that the steep bathymetric escarpment SE of Rhodes is maintained through faulting, it is reasonable to assume that the fault responsible has this strike and slip vector.

However, since this slip vector differs significantly from the direction of convergence between Rhodes and Nubia measured using GPS data (195°; see main text), if the fault uplifting Rhodes is a "pure" reverse fault it is necessary to infer the presence of an additional fault with a strike-slip component.

To test whether such an additional fault is necessary, we fixed the horizontal slip vector at 195° (adjusting rake accordingly depending on strike and dip) and allowed other parameters to vary freely. The results of this grid search are shown in Figure S5.

Note that although the minimum misfit is lower for models G-I (Figure 6, main text) on this plot than in Table 2 (main text), this is a result of running the grid search for a wide range of parameter space (up to 90 km length, for example), whereas models G-I were chosen because their lengths were comparable to those in models A-F. The same arguments for preferring a "pure" reverse fault over models G-I also apply for the lower-misfit models in Figure S5.

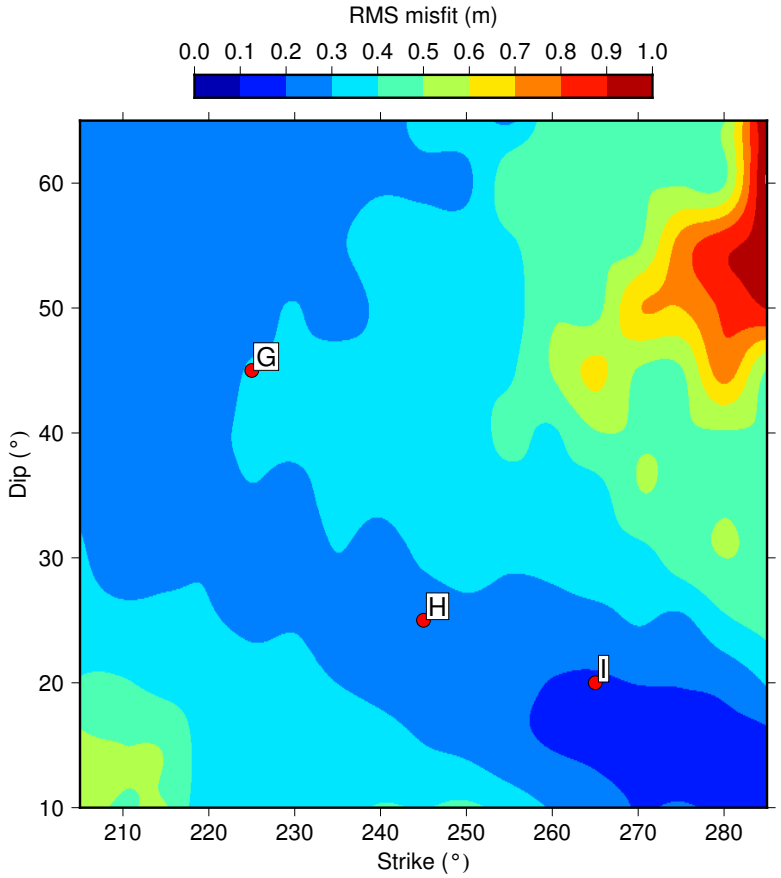

Figure S5: Variation of minimum RMS misfit with strike and dip, with horizontal azimuth of slip vector fixed at 195° and all other parameters free to vary within the limits in Table 1 (main text). Letters show the locations in parameter space of models G-I (Figure 6, main text).